

# Origin of magnetic field in compact stars and magnetic properties of quark matter

T. Tatsumi<sup>1</sup>, T. Maruyama<sup>2</sup>, K. Nawa<sup>1</sup> and E. Nakano<sup>3,4</sup>

<sup>1</sup> Department of Physics, Kyoto University, Kyoto 606-8502, Japan;  
*tatsumi@ruby.scphys.kyoto-u.ac.jp; nawa@ruby.scphys.kyoto-u.ac.jp*

<sup>2</sup> College of Bioresource Science, Nihon University, Fujisawa 252-8510,  
Japan;*tomo@brs.nihon-u.ac.jp*

<sup>3</sup> Department of Physics, Tokyo Metropolitan University, 1-1 Minami-Ohsawa, Hachioji,  
Tokyo 192-0397, Japan

<sup>4</sup> Yukawa Institute for Theoretical Physics, Kyoto University, Kyoto 606-8502,  
Japan;*enakano@yukawa.kyoto-u.ac.jp*

## Abstract

Microscopic origin of the magnetic field observed in compact stars is studied in quark matter. Spontaneous spin polarization appears in high-density region due to the Fock exchange term. On the other hand, quark matter becomes unstable to form spin density wave in the moderate density region, where restoration of chiral symmetry plays an important role. Coexistence of the magnetism and color superconductivity is briefly discussed.

## 1 Introduction

Nowadays it is widely accepted that there should be realized various phases of QCD in temperature ( $T$ ) - density ( $\rho_B$ ) plane. When we emphasize the low  $T$  and high  $\rho_B$  region, the subjects are sometimes called high-density QCD. The main purposes in this field should be to figure out the new phases and their properties, and to extract their symmetry breaking pattern and low-energy excitation modes there on the basis of QCD. On the other hand, these studies have phenomenological implications on relativistic heavy-ion collisions and compact stars like neutron stars or quark stars.

In this lecture we'd like to address magnetic properties of quark matter. We shall see various types of magnetic ordering may be expected in quark matter at finite density or temperature. They arise due to the quark particle-hole ( $p - h$ ) correlations in the pseudo-scalar or axial-vector channel. We first discuss the ferromagnetic phase transition and then another magnetic feature in the second part.

Phenomenologically the concept of magnetism should be directly related to the origin of strong magnetic field observed in compact stars [1]; e.g., it amounts to  $O(10^{12}\text{G})$  at the surface of radio pulsars. Recently a new class of pulsars called magnetars has been discovered with super strong magnetic field,  $B_s \sim 10^{14-15}\text{G}$ , estimated from the  $P - \dot{P}$  curve [2]. First observations are indirect evidences for super strong magnetic field, but discoveries of some

absorption lines stemming from the cyclotron frequency of protons have been currently reported [3].

The origin of the strong magnetic field has been a long standing problem since the first pulsar was discovered [1]. A naive working hypothesis is the conservation of the magnetic flux and its squeezing during the evolution from a main-sequence progenitor star to a compact star,  $B \propto R^{-2}$  with  $R$  being the radius. Taking the sun as a typical one, we have  $B \sim 10^3\text{G}$  and  $R \sim 10^{10}\text{cm}$ . If it is squeezed to a typical radius of usual neutron stars,  $R \sim 10\text{km}$ , the conservation of the magnetic flux gives  $10^{11}\text{G}$ , which is consistent with the observations for radio pulsars. However, we find  $R \sim 100\text{m}$  to explain  $B \sim 10^{15}\text{G}$  observed for magnetars, which leads to a contradiction since the Schwatzschild radius is  $O(1\text{km})$  much larger than  $R$ .

Since there should be developed hadronic matter inside compact stars, it would be reasonable to consider a microscopic origin of such strong magnetic field: ferromagnetism or spin polarization is one of the candidates to explain it. Makishima also suggested the hadronic origin of the magnetic field observed in binary X-ray pulsars [4].

When we consider the magnetic-interaction energy by a simple formula,  $E_{\text{mag}} = \mu_i B$  with the magnetic moment,  $\mu_i = e_i/(2m_i)$ , we can easily estimate it for  $B = O(10^{15}\text{G})$ ; it amounts to several MeV for electrons, while several keV for nucleons and 10 - 100 keV for quarks. This simple consideration may imply that strong interaction gives a feasible origin for the strong magnetic field, since its typical energy scale is MeV. The possibility of ferromagnetism in nuclear matter has been elaborately studied since the first pulsars were observed, but negative results have been reported so far [5]. In the first part of this lecture, we consider its possibility in quark matter from a different point of view [6].

In the second part we discuss another magnetic aspect in quark matter at moderate densities, where the QCD interaction is still strong and some non-perturbative effects still remain. One of the most important features observed there is restoration of chiral symmetry; the blocking of  $\bar{q}q$  excitations due to the existence of the Fermi sea gives rise to restoration of chiral symmetry at a certain density and many people believe that deconfinement transition also occurs at almost the same time. There have been proposed various types of the  $p$ - $h$  condensations at moderate densities [7, 8], in which the  $p$ - $h$  pair in scalar or tensor channel has the finite total momentum indicating standing waves (the chiral density waves). The instability for the density wave in quark matter was first discussed by Deryagin *et al.* [7] at asymptotically high densities where the interaction is very weak, and they concluded that the density-wave instability prevails over the BCS one in the large  $N_c$  (the number of colors) limit due to the dynamical suppression of colored BCS pairings.

In general, density waves are favored in 1-D (one spatial dimension) systems and have the wave number  $Q = 2k_F$  according to the Peierls instability [9], e.g., charge density waves (CDW) in quasi-1-D metals. The essence of its mechanism is the nesting of Fermi surfaces and the level repulsion (crossing) of single particle spectra due to the interaction for the finite wave number. Thus the low dimensionality has an essential role to produce the density-wave states. In the higher dimensional systems, however, the transitions occur provided the interaction of a corresponding ( $p$ - $h$ ) channel is strong enough. For the 3-D electron gas, it was shown by Overhauser [10] that paramagnetic state is unstable with respect to the formation of the static spin density wave (SDW), in which spectra of up- and down-spin states are deformed to bring about the level crossing due to the spin exchange interactions,

while the wave number does not precisely coincide with  $2k_F$  because of the incomplete nesting in higher dimension.

We shall see a kind of spin density wave develops there, in analogy with SDW mentioned above.. It occurs along with the chiral condensation and is represented by a dual standing wave in scalar and pseudo-scalar condensates (we have called it ‘dual chiral-density wave’, DCDW). DCDW has different features in comparison with the previously discussed chiral density waves [7, 8]. One outstanding feature concerns its magnetic aspect; DCDW induces *spin density wave*.

## 2 Ferromagnetism in QCD

### 2.1 A heuristic argument

Quark matter bears some resemblance to electron gas interacting with the Coulomb potential; the gluon exchange interaction in QCD has some resemblance to the Coulomb interaction in QED, and color neutrality of quark matter corresponds to charge neutrality of electron gas under the background of positively charged ions.

It was Bloch who first suggested a mechanism leading to ferromagnetism of itinerant electrons [11]. The mechanism is very simple but largely reflects the Fermion nature of electrons. Since there works no direct interaction between electrons as a whole, the Fock exchange interaction gives a leading contribution. Then it is immediately conceivable that a most attractive channel is the parallel spin pair, whereas the anti-parallel pair gives null contribution (see Eq. (5) below). This is nothing but a consequence of the Pauli exclusion principle: electrons with the same spin polarization cannot closely approach to each other, which effectively avoid the Coulomb repulsion. On the other hand a polarized state should have a larger kinetic energy by rearranging the two Fermi spheres. Thus there is a trade-off between the kinetic and interaction energies, which leads to a *spontaneous spin polarization (SSP)* or FM at some density. One of the essential points we learned here is that we need no spin-dependent interaction in the original Lagrangian to see SSP.

Then it might be natural to ask how about in QCD. We list here some features of QCD related to this subject. (1) the quark-gluon interaction in QCD is rather simple, compared with the nuclear force; it is a gauge interaction like in QED. (2) quark matter should be a color neutral system and only the *Fock exchange* interaction is also relevant like in the electron system. (3) there is an additional flavor degree of freedom in quark matter; gluon exchange never change flavor but it comes in through the generalized Pauli principle. (4) quarks should be treated relativistically, different from the electron system.

The last feature requires a new definition and formulation of SSP or FM in relativistic systems since “spin” is no more a good quantum number in relativistic theories; spin couples with momentum and its direction changes during the motion. It is well known that the Pauli-Lubanski vector  $W^\mu$  is the four vector to represent the spin degree of freedom in a covariant form; the spinor of the free Dirac equation is the eigenstate of the operator,

$$W \cdot a = -\frac{1}{2}\gamma_5 \not{a} \not{k}, \quad (1)$$

where a 4-axial-vector  $a^\mu$  s.t.

$$\mathbf{a} = \boldsymbol{\zeta} + \frac{\mathbf{k}(\boldsymbol{\zeta} \cdot \mathbf{k})}{m(E_k + m)}, \quad a^0 = \frac{\mathbf{k} \cdot \boldsymbol{\zeta}}{m} \quad (2)$$

with the axial vector  $\boldsymbol{\zeta}$ . We can see that  $a^\mu$  is reduced to a three vector  $(0, \boldsymbol{\zeta})$  in the rest frame, where we can allocate  $\boldsymbol{\zeta} = (0, 0, \pm 1)$  to spin ‘‘up’’ and ‘‘down’’ states. Thus we can still use  $\boldsymbol{\zeta}$  to specify the two intrinsic polarized states even in the general Lorentz frame.

The Fock exchange interaction,  $f_{\mathbf{k}\boldsymbol{\zeta}, \mathbf{q}\boldsymbol{\zeta}'}$ , between two quarks is then given by

$$f_{\mathbf{k}\boldsymbol{\zeta}, \mathbf{q}\boldsymbol{\zeta}'} = g^2 \frac{m}{E_k} \frac{m}{E_q} \frac{2}{9m^2} [2m^2 - \mathbf{k} \cdot \mathbf{q} - m^2 \mathbf{a} \cdot \mathbf{b}] \frac{1}{(k - q)^2}, \quad (3)$$

in the lowest order, where the spin dependent term renders

$$\begin{aligned} a \cdot b &= -\frac{1}{m_q^2} \left[ -(\mathbf{k} \cdot \boldsymbol{\zeta})(\mathbf{q} \cdot \boldsymbol{\zeta}') + m^2 \boldsymbol{\zeta} \cdot \boldsymbol{\zeta}' \right. \\ &+ \{m(E_k + m)(\boldsymbol{\zeta} \cdot \mathbf{q})(\boldsymbol{\zeta}' \cdot \mathbf{q}) + m(E_q + m)(\boldsymbol{\zeta}' \cdot \mathbf{k})(\boldsymbol{\zeta} \cdot \mathbf{k}) \\ &+ (\mathbf{k} \cdot \mathbf{q})(\boldsymbol{\zeta} \cdot \mathbf{k})(\boldsymbol{\zeta}' \cdot \mathbf{q})\} / (E_k + m)(E_q + m) \left. \right]. \end{aligned} \quad (4)$$

It exhibits a complicated spin-dependent structure arising from the Dirac four spinor, while it is reduced to a simple form,

$$-\frac{2}{9} g^2 \frac{1 + \boldsymbol{\zeta} \cdot \boldsymbol{\zeta}'}{(\mathbf{k} - \mathbf{q})^2} \quad (5)$$

in the non-relativistic limit as in the electron system. Eq. (5) clearly shows why parallel spin pairs are favored, while we cannot see it clearly in the relativistic expression (4). We have explicitly demonstrated that the ferromagnetic phase should be realized at relatively low density region [6]: quark matter is spontaneously polarized at low densities like the electron gas. The phase transition is of first order and the critical density is around the nuclear density for quark mass  $m_q \simeq 300\text{MeV}$  and coupling constant  $\alpha_c \sim 2.2$ , which are used in the MIT bag model. It should be interesting to see a recent reference [14], where the author also found the ferromagnetic phase transition at low densities within the perturbative QCD calculation beyond the lowest-order diagram.

## 2.2 Self-consistent calculation

If we understand FM or magnetic properties of quark matter more deeply, we must proceed to a self-consistent approach, like the Hartree-Fock theory, beyond the previous perturbative argument.

We begin with an OGE action:

$$I_{int} = -g^2 \frac{1}{2} \int d^4x \int d^4y \left[ \bar{\psi}(x) \gamma^\mu \frac{\lambda_a}{2} \psi(x) \right] D_{\mu\nu}(x, y) \left[ \bar{\psi}(y) \gamma^\nu \frac{\lambda_a}{2} \psi(y) \right], \quad (6)$$

where  $D^{\mu\nu}$  denotes the gluon propagator. By way of the mean-field approximation, we have

$$I_{MF} = \int \frac{d^4p}{(2\pi)^4} \bar{\psi}(p) G_A^{-1}(p) \psi(p). \quad (7)$$

The inverse quark Green function  $G^{-1}(p)$  involves various self-energy (mean-field) terms, of which we only keep the color singlet particle-hole mean-field  $V(p)$ ,

$$G_A(p)^{-1} = \not{p} - m + \not{\mu} + V(p). \quad (8)$$

Taking into account the lowest diagram, we can then write down the self-consistent equations for the mean-field,  $V$ :

$$-V(k) = (-ig)^2 \int \frac{d^4p}{i(2\pi)^4} \{-iD^{\mu\nu}(k-p)\} \gamma_\mu \frac{\lambda_\alpha}{2} \{-iG_A(p)\} \gamma_\nu \frac{\lambda_\alpha}{2}. \quad (9)$$

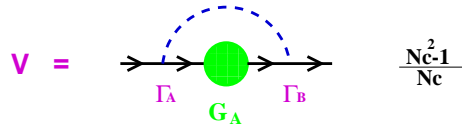


Figure 1: Graphical interpretations of the equation (9) with coefficient in front of R.H.S. given by  $N_c$ .

Applying the Fierz transformation for the OGE action (6) we can see that there appear the color-singlet scalar, pseudo-scalar, vector and axial-vector self-energies by the Fock exchange interaction. In general we must take into account these self-energies in  $V$ ,  $V = U_s + \gamma_5 U_{ps} + \gamma_\mu U_v^\mu + \gamma_\mu \gamma_5 U_{av}^\mu$  with the mean-fields  $U_i$ . Here we retain only  $U_s, U_v^0, U_{av}^3$  in  $V$  and suppose that others to be vanished.

**Problem:** Show that there is no tensor mean-field as a consequence of chiral symmetry in (6).

According to the above assumptions and considerations the mean-field  $V$  in Eq.(8) renders

$$V = \gamma_3 \gamma_5 U_A, \quad U_A \equiv U_{av}^3, \quad (10)$$

with the axial-vector mean-field  $U_A$ <sup>1</sup>.

The poles of  $G_A(p)$ ,  $\det G_A^{-1}(p_0 = \epsilon_n) = 0$ , give the single-particle energy spectrum:

$$\epsilon_n = \pm \epsilon_\pm \quad (11)$$

$$\epsilon_\pm = \sqrt{\mathbf{p}^2 + \mathbf{U}_A^2 + m^2 \pm 2\sqrt{m^2 \mathbf{U}_A^2 + (\mathbf{p} \cdot \mathbf{U}_A)^2}}, \quad (12)$$

where the subscript  $\pm$  in the energy spectrum represents spin degrees of freedom, and the dissolution of the degeneracy corresponds to the *exchange splitting* of different “spin” states [12].

There are two Fermi seas with different volumes for a given quark number due to the exchange splitting in the energy spectrum. The appearance of the rotation symmetry breaking

<sup>1</sup>Since the scalar and vector mean-fields only renormalize the mass and the quark-number chemical potential, respectively, we discard them here for simplicity.

term,  $\propto \mathbf{p} \cdot \mathbf{U}_A$  in the energy spectrum implies deformation of the Fermi sea: thus rotation symmetry is violated in the momentum space as well as the coordinate space,  $O(3) \rightarrow O(2)$ . Accordingly the Fermi sea of majority quarks exhibits a “prolate” shape ( $F^-$ ), while that of minority quarks an “oblate” shape ( $F^+$ ) as seen Fig. 2.

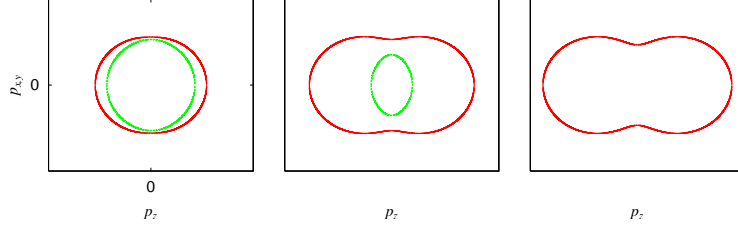


Figure 2: Modification of the Fermi sea as  $U_A$  is increased from left to right. The larger Fermi sea ( $F^-$ ) takes a prolate shape, while the smaller one ( $F^+$ ) an oblate shape for a given  $U_A$ . In the large  $U_A$  limit (completely polarized case),  $F^+$  disappears as in the right panel.

Here we demonstrate some numerical results; we replaced the original OGE by the “contact” interaction,  $D^{\mu\nu} \rightarrow -g^{\mu\nu}/\Lambda^2$ . Then the self-consistent equation can be written as

$$U_A = -\frac{N_c^2 - 1}{4N_c} \tilde{g}^2 \int \frac{d^3p}{(2\pi)^3} \sum_s \theta(\mu - \epsilon_s(\mathbf{p})) \frac{U_A + s\beta_p}{\epsilon_s(\mathbf{p})}, \quad (13)$$

within the “contact” interaction,  $\tilde{g}^2 \equiv g^2/\Lambda^2$ . Note that the expression for  $U_A$ , Eq. (13), is nothing but the simple sum of the expectation value of the spin operator over the Fermi seas.

### 2.3 Phase diagram in temperature-density plane

We will present the phase diagram in the three-flavor case under mainly two conditions [15]: the chemical equilibrium condition (CEC)  $\mu_u = \mu_d = \mu_s$  and the charge neutral condition without electrons (CNC)  $\rho_u = \rho_d = \rho_s$ , where quark masses are taken as  $m_u = m_d = 5\text{MeV}$  and  $m_s = 150 - 350\text{MeV}$ , i.e.,  $\mu_s = \sqrt{\mu_{u,d}^2 + m_s^2 - m_{u,d}^2}$  for  $T = 0$ . In both conditions, since the spin polarization caused by the axial-vector mean-field is fully enhanced by the quark masses, choice of the current quark mass affects the results, especially, the strange quark mass is large, and therefore has essential effect on the spin polarization. To get the phase diagram, we use the thermodynamic potential  $\Omega$  within the mean-field approximation,

$$\begin{aligned} \Omega = & -N_c \sum_{u=\pm 1} \sum_{s=\pm} \sum_{i=u,d,s} \int \frac{d^3\mathbf{k}}{(2\pi)^3} T \log \left\{ \exp \left[ -\frac{\epsilon_s(\mathbf{k}, m_i, U_A) - u\mu_i}{T} \right] + 1 \right\} \\ & - N_c \sum_{s=\pm} \sum_{i=u,d,s} \int \frac{d^3\mathbf{k}}{(2\pi)^3} \epsilon_s(\mathbf{k}, m_i, U_A) + \frac{U_A^2}{4\tilde{g}^2}. \end{aligned} \quad (14)$$

The second term is the vacuum contribution and can be regularized by ,e.g., the proper-time method. We can see that the potential  $U_A$  reproduces the self-consistent equation Eq. (13) in the three-flavor case.

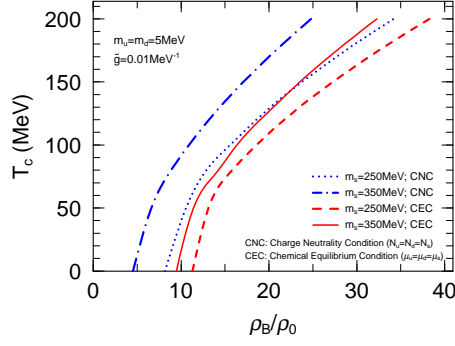


Figure 3: Phase diagram for two cases of strange quark masses, 250, 350MeV.

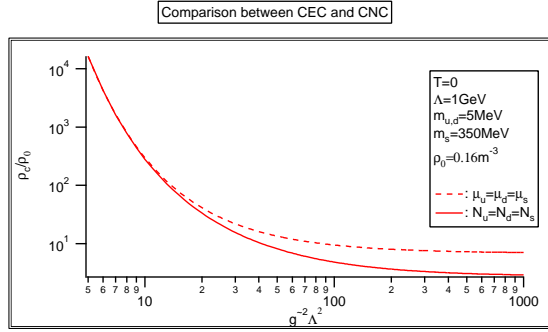


Figure 4: Critical density as a function of  $\tilde{g}$  under two conditions: CEC and CNC.

Fig. 3 shows the resulting phase diagram under the two conditions mentioned above; CEC and CNC.

The figure shows the critical temperature (the Curie temperature) for a given baryon density, CNC tends to facilitate the system being the spin polarization than CEC. This is because CNC holds the larger strange-quark density in comparison with CEC.

Since the axial-vector mean-field comes from the Fock exchange interaction and causes a kind of particle-hole condensation, which is enhanced by the Fermi sea contribution, there exists a critical density for a given coupling constant  $\tilde{g}$ . We show the critical density by varying the effective coupling constant  $\tilde{g}$  in Fig. 4. The critical density lowers with the larger coupling strength, and this tendency is enhanced in the case of CNC. The result also indicates that even for the weak-coupling regime in QCD, the spin polarization may appear in sufficiently large densities at sufficiently low temperature.

## 2.4 Color magnetic superconductivity

If FM is realized in quark matter, it might be in the color superconducting (CSC) phase [16, 17]. In this section we briefly discuss a possibility of the coexistence of FM and CSC, which we call *Color magnetic superconductivity* [18]. In passing, it would be worth mentioning the corresponding situation in condensed matter physics. Magnetism and superconductivity (SC) have been two major concepts in condensed matter physics and their interplay has been

repeatedly discussed [19]. Very recently some materials have been observed to exhibit the coexistence phase of FM and SC [20]. In our case we shall see somewhat different features, but the similar aspects as well.

We begin with the OGE action (7) and extend it to include the quark pairings. We consider the quark pairings on the same Fermi surfaces  $F^\pm$  by using the eigenspinors  $\phi_s$ ,  $s = \pm 1$  with the energy (12); the pairing function then reads

$$\Delta(\mathbf{p}) = \sum_{s=\pm} \tilde{\Delta}_s(\mathbf{p}) B_s(\mathbf{p}), \quad B_s(\mathbf{p}) = \gamma_0 \phi_{-s}(\mathbf{p}) \phi_s^\dagger(\mathbf{p}). \quad (15)$$

The structure of the gap function (15) is inferred from a physical consideration of a quark pair as in the usual BCS theory: we consider here the quark pair on each Fermi surface with opposite momenta,  $\mathbf{p}$  and  $-\mathbf{p}$  so that they result in a linear combination of  $J^\pi = 0^-, 1^-$ .  $\tilde{\Delta}_s$  is still a matrix in the color-flavor space. Taking into account the property that the most attractive channel of the OGE interaction is the color antisymmetric  $\bar{3}$  state, the quark pair must be in the flavor singlet state. Thus we can choose the form of the gap function as

$$\left(\tilde{\Delta}_s\right)_{\alpha\beta;ij} = \epsilon^{\alpha\beta 3} \epsilon^{ij} \Delta_s \quad (16)$$

for the two-flavor case (2SC), where  $\alpha, \beta$  denote the color indices and  $i, j$  the flavor indices. In refs. [18] we can see that the gap functions  $\Delta_s$  have a polar angle ( $\theta$ ) dependence on the Fermi surfaces: both the gap functions have nodes at poles ( $\theta = 0, \pi$ ) and take the maximal values at the vicinity of equator ( $\theta = \pi/2$ ), keeping the relation,  $\Delta_- \geq \Delta_+$ . This feature is very similar to  ${}^3P$  pairing in liquid  ${}^3\text{He}$  or nuclear matter [21, 22]; actually we can see our pairing function Eq. (16) to exhibit an effective  $P$  wave nature by a genuine relativistic effect by the Dirac spinors. As a consequence, we can say that FM and CSC barely interfere with each other [18].

## 3 Dual chiral density wave

### 3.1 Chiral symmetry restoration and Instability of the directional mode

We consider here another type of density wave described as a dual standing wave in the scalar and pseudo-scalar mean-fields [23]. It is well known that chiral symmetry is spontaneously broken (SSB) due to the quark-anti-quark condensate in the vacuum and at low densities; both the scalar and pseudo-scalar densities always reside on the chiral circle of the finite modulus, and any chiral transformation by a chiral angle  $\theta$  shifts each value on the circle, while the QCD Lagrangian is invariant for constant  $\theta$ .

The spatially variant chiral angle  $\theta(\mathbf{r})$  represents the degree of freedom of the Nambu-Goldstone mode in the SSB vacuum. The dual chiral density wave (DCDW) is described by such a chiral angle  $\theta(\mathbf{r})$ . When the chiral angle has some space-time dependence, there should appear extra terms in the effective potential: one trivial term is the one describing the quark and DCDW coupling due to the non-commutability of  $\theta(\mathbf{r})$  with the kinetic (differential) operator in the Dirac operator. Another one is nontrivial and comes from the quantum effect: the energy spectrum of the quark is modified in the presence of  $\theta(\mathbf{r})$  and thereby the

vacuum energy has an additional term,  $\propto (\nabla\theta)^2$  in the lowest order. This can be regarded as an appearance of the kinetic term for DCDW through the vacuum polarization [24].

### 3.2 DCDW in the NJL model

Taking the Nambu-Jona-Lasinio (NJL) model as a simple but nontrivial example, we explicitly demonstrate that quark matter becomes unstable for a formation of DCDW above a critical density; the NJL model has been recently used as an effective model of QCD, embodying spontaneous breaking of chiral symmetry in terms of quark degree of freedom [28]<sup>2</sup>. We shall explicitly see the DCDW state exhibits a ferromagnetic property.

We start with the NJL Lagrangian with  $N_f = 2$  flavors and  $N_c = 3$  colors,

$$\mathcal{L}_{NJL} = \bar{\psi}(i\cancel{\partial} - m_c)\psi + G[(\bar{\psi}\psi)^2 + (\bar{\psi}i\gamma_5\boldsymbol{\tau}\psi)^2], \quad (17)$$

where  $m_c$  is the current mass,  $m_c \simeq 5\text{MeV}$ . Under the Hartree approximation, we linearize Eq. (17) by partially replacing the bilinear quark fields by their expectation values with respect to the ground state.

In the usual treatment to study the restoration of chiral symmetry at finite density, authors implicitly discarded the pseudo-scalar mean-field, while this is justified only for the vacuum of a definite parity. We assume here the following mean-fields,

$$\begin{aligned} \langle \bar{\psi}\psi \rangle &= \Delta \cos(\mathbf{q} \cdot \mathbf{r}) \\ \langle \bar{\psi}i\gamma_5\tau_3\psi \rangle &= \Delta \sin(\mathbf{q} \cdot \mathbf{r}), \end{aligned} \quad (18)$$

and others vanish<sup>3</sup>. Accordingly, we define a new quark field  $\psi_W$  by the Weinberg transformation,

$$\psi_W = \exp[i\gamma_5\tau_3\mathbf{q} \cdot \mathbf{r}/2]\psi, \quad (19)$$

to separate the degrees of freedom of the amplitude and phase of DCDW in the Lagrangian. In terms of the new field the effective Lagrangian renders

$$\mathcal{L}_{MF} = \bar{\psi}_W[i\cancel{\partial} - M - 1/2\gamma_5\tau_3\cancel{q}]\psi_W - G\Delta^2, \quad (20)$$

where we put  $M \equiv -2G\Delta$  and  $q^\mu = (0, \mathbf{q})$ , taking the chiral limit ( $m_c = 0$ ). The form given in (20) appears to be the same as the usual one, except the axial-vector field generated by the wave vector of DCDW; the *amplitude* of DCDW produces the dynamical quark mass in this case. We shall see the wave vector  $\mathbf{q}$  is related to the magnetization: the *phase* of DCDW induces the magnetization.

---

<sup>2</sup>We can see that the OGE interaction gives the same form after the Fierz transformation in the zero-range limit [18]

<sup>3</sup>It would be interesting to recall that the DCDW configuration is similar to pion condensation in high-density nuclear matter within the  $\sigma$  model, considered by Dautry and Nyman (DN)[25, 26], where  $\sigma$  and  $\pi^0$  meson condensates take the same form as Eq. (18). The same configuration has been also assumed for non-uniform chiral phase in hadron matter by the use of the Nambu-Jona-Lasinio model [27]. However, DCDW is by no means the pion condensation but should be directly considered as particle-hole and particle-antiparticle quark condensation in the deconfinement phase.

Using Eq. (20), we can find a spatially uniform solution,  $\psi_W = u_W(p) \exp(i\mathbf{p} \cdot \mathbf{r})$ , with the eigenvalues,

$$E_p^\pm = \sqrt{E_p^2 + |\mathbf{q}|^2/4 \pm \sqrt{(\mathbf{p} \cdot \mathbf{q})^2 + M^2|\mathbf{q}|^2}}, \quad E_p = (M^2 + |\mathbf{p}|^2)^{1/2} \quad (21)$$

for positive-energy (valence) quarks with different spin polarizations (c.f. (12)).

### 3.3 Thermodynamic potential

The thermodynamic potential is given as

$$\begin{aligned} \Omega_{\text{total}} &= \gamma \int \frac{d^3p}{(2\pi)^3} [(E_p^- - \mu)\theta_- + (E_p^+ - \mu)\theta_+] - \gamma \int \frac{d^3p}{(2\pi)^3} [E_p^- + E_p^+] + M^2/4G \\ &\equiv \Omega_{\text{val}} + \Omega_{\text{vac}} + M^2/4G. \end{aligned} \quad (22)$$

where  $\theta_\pm = \theta(\mu - E_p^\pm)$ ,  $\mu$  is the chemical potential and  $\gamma$  the degeneracy factor  $\gamma = N_f N_c$ . The first term  $\Omega_{\text{val}}$  is the contribution by the valence quarks filled up to the chemical potential, while the second term  $\Omega_{\text{vac}}$  is the vacuum contribution that is apparently divergent. We shall see both contributions are *indispensable* in our discussion. Once  $\Omega_{\text{total}}$  is properly evaluated, the equations to be solved to determine the optimal values of  $\Delta$  and  $q$  are

$$\frac{\delta\Omega_{\text{total}}}{\delta\Delta} = \frac{\delta\Omega_{\text{total}}}{\delta q} = 0. \quad (23)$$

Since NJL model is not renormalizable, we need some regularization procedure to get a meaningful finite value for the vacuum contribution  $\Omega_{\text{vac}}$ , which can be recast in the form,

$$\Omega_{\text{vac}} = i\gamma \int \frac{d^4p}{(2\pi)^4} \text{tr} \ln S_W, \quad (24)$$

with use of the propagator  $S_W = (\not{p} - M - 1/2\tau_3\gamma_5\not{q})^{-1}$ . Since the energy spectrum is no more rotation symmetric, we cannot apply the usual momentum cut-off regularization (MCOR) scheme to regularize  $\Omega_{\text{vac}}$ <sup>4</sup>. Instead, we adopt the proper-time regularization (PTR) scheme [29]. Introducing the proper-time variable  $\tau$ , we eventually find

$$\Omega_{\text{vac}} = \frac{\gamma}{8\pi^{3/2}} \int_0^\infty \frac{d\tau}{\tau^{5/2}} \int_{-\infty}^\infty \frac{dp_z}{2\pi} \left[ e^{-(\sqrt{p_z^2 + M^2 + q/2})^2 \tau} + e^{-(\sqrt{p_z^2 + M^2 - q/2})^2 \tau} \right] - \Omega_{\text{ref}}, \quad (25)$$

which is reduced to the standard formula [28] in the limit  $q \rightarrow 0$ .

The integral with respect to the proper time  $\tau$  is not well defined as it is, since it is still divergent due to the  $\tau \sim 0$  contribution. Regularization proceeds by replacing the lower bound of the integration range by  $1/\Lambda^2$ , which corresponds to the momentum cut-off in the MCOR scheme.

---

<sup>4</sup>We would like to stress that the regularization should be, at least, independent of  $\Delta$  and  $q$ . Otherwise it is inconsistent with Eq. (23).

Now we examine a possible instability of quark matter with respect to formation of DCDW. In the following we first consider the sign change of the curvature of  $\Omega_{\text{total}}$  at the origin (*stiffness* parameter),  $\beta$ . Expanding  $\Omega_{\text{vac}}$  with respect to  $q$  up to  $O(q^2)$ , we find

$$\begin{aligned}\Omega_{\text{vac}} &= \Omega_{\text{vac}}^0 + \frac{\gamma\Lambda^2}{16\pi^2} J(M^2/\Lambda^2)q^2 + O(q^4) \\ &\equiv \Omega_{\text{vac}}^0 + \Omega_{\text{vac}}^{\text{mag}} + O(q^4),\end{aligned}\tag{26}$$

where  $J(x)$  is a universal function,  $J(x) = -x\text{Ei}(-x)$ , with the exponential integral  $\text{Ei}(-x)$ .  $\Omega_{\text{vac}}^{\text{mag}}$  is the pure magnetic contribution and provides a kinetic term ( $\propto (\nabla\theta)^2$ ) for DCDW. It originates from a vacuum polarization effect in the presence of DCDW and gives a 'repulsive' (positive) contribution, so that the vacuum is stable against formation of DCDW. Note that it gives a null contribution in case of  $M = 0$ , irrespective of  $q$ , as it should be.

The coefficient of  $q^2$  term in  $\Omega_{\text{vac}}^{\text{mag}}$ , the vacuum stiffness parameter,  $\beta_{\text{vac}}$ , has a definite physical meaning. Since the pion decay constant  $f_\pi$  is mass dependent and is given in terms of  $J(x)$  within the NJL model [28],  $\beta_{\text{vac}}$  can be written as  $\beta_{\text{vac}} = \frac{1}{2}f_\pi^2$ .

For given  $\mu, M$  and  $q$  we can evaluate the valence contribution  $\Omega_{\text{val}}$  using Eq. (21), but its general formula is very complicated. However, it may be sufficient to consider the small  $q$  case for our present purpose. Then the thermodynamic potential can be expressed as  $\Omega_{\text{val}} = \epsilon_{\text{val}}(q) - \mu\rho_{\text{val}}(q)$ , where  $\epsilon_{\text{val}}(q)$  and  $\rho_{\text{val}}(q)$  are the energy density and the quark-number density, respectively. Expanding  $\epsilon_{\text{val}}(q)$  up to the  $O(q^2)$  we find

$$\epsilon_{\text{val}}(q) \simeq \epsilon_{\text{val}}^0 + \frac{\gamma}{8\pi^2} M^2 q^2 \left[ \frac{\mu}{\sqrt{\mu^2 - M^2}} - \ln \frac{\mu + \sqrt{\mu^2 - M^2}}{M} \right] + O(q^4)\tag{27}$$

with  $\epsilon_{\text{val}}^0 = \gamma/8\pi^2 \left[ \mu\sqrt{\mu^2 - M^2} (2\mu^2 - M^2) - M^4 \ln(\mu + \sqrt{\mu^2 - M^2}/M) \right]$  for normal quark matter without DCDW. Thus the valence contribution can be finally written as

$$\begin{aligned}\Omega_{\text{val}} &= \Omega_{\text{val}}^0 - \frac{\gamma}{8\pi^2} M^2 q^2 H(\mu/M) + O(q^4) \\ &\equiv \Omega_{\text{val}}^0 + \Omega_{\text{val}}^{\text{mag}} + O(q^4)\end{aligned}\tag{28}$$

up to  $O(q^2)$ , where  $H(x) = \ln(x + \sqrt{x^2 - 1})$  and  $\Omega_{\text{val}}^0 = \epsilon_{\text{val}}^0 - \mu\rho_{\text{val}}^0$  with  $\rho_{\text{val}}^0 = \frac{\gamma}{3\pi^2}(\mu^2 - M^2)^{3/2}$  for normal quark matter. The valence stiffness parameter then reads

$$\beta_{\text{val}} = -\frac{\gamma}{8\pi^2} M^2 H(\mu/M)\tag{29}$$

Since the function  $H(x)$  is always positive and accordingly  $\beta_{\text{val}} \leq 0$ , the magnetic term  $\Omega_{\text{val}}^{\text{mag}}$  always gives a negative energy and approaches to zero as  $M \rightarrow 0$  (triviality).

We may easily understand why the valence quarks always favor the formation of DCDW. First, consider the energy spectra for massless quarks (see Fig. 5).

As is already discussed, our theory becomes trivial in this case and we find two spectra

$$E_p^\pm = \sqrt{p_\perp^2 + (|p_z| \pm q/2)^2}, \quad \mathbf{p}_\perp = (p_x, p_y, 0),\tag{30}$$

which are essentially equivalent to  $E_p^\pm = |\mathbf{p}|$ .

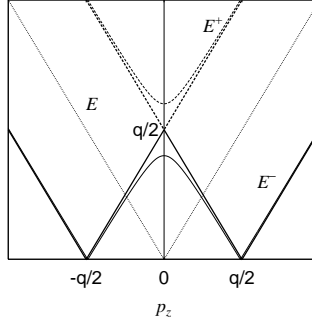


Figure 5: Energy spectra for  $\mathbf{p}_\perp = 0$ .  $E^\pm$  with  $M = 0$  (thick solid and dashed lines).  $\tilde{E}^\pm$  with the definite chirality is also shown for comparison (dotted line). We can see there is a degeneracy of  $E^\pm$  at  $p_z = 0$  for  $M = 0$ , while it is resolved by the mass (thin solid and dashed lines).

**Problem:** Construct the eigenstates of chirality  $\gamma_5$  by taking the linear combination of  $\psi_W^\pm$ . Their spectra are given by  $\tilde{E}^\pm = \sqrt{p_\perp^2 + (p_z \pm q/2)^2}$ .

There is a level crossing at  $\mathbf{p} = \mathbf{0}$ . Once the mass term is taken into account this degeneracy is resolved and the exchange splitting appears there. Hence it causes an energy gain, if  $q = O(2\mu)$ ; we can see that this mechanism is very similar to that of SDW by Overhauser [8, 10].

Using Eqs. (22), (26), (28) we write the thermodynamic potential as

$$\Omega_{\text{total}} = \Omega_{NJL} + \beta q^2 + O(q^4) \quad (31)$$

with the total stiffness parameter  $\beta = \beta_{vac} + \beta_{val}$  and the usual NJL expression without DCDW,  $\Omega_{NJL} = \Omega_{vac}^0(M) + \Omega_{val}^0(M) + M^2/4G$ . The dynamical quark mass  $M$  is given by the equation,  $\partial\Omega_{\text{total}}/\partial M = 0$ ; At the order of  $q^0$  the dynamical quark mass  $M^0$  is determined by the equation,  $\partial\Omega_{NJL}/\partial M|_{M^0} = 0$ . Since  $M - M^0 = O(q^2)$ , DCDW onsets at a certain density where the total stiffness parameter  $\beta$  becomes negative: the critical chemical potential  $\mu^{cr}$  is determined by the equation,

$$\beta = \frac{1}{2}f_\pi^2 - \frac{\gamma}{8\pi^2} (M^0)^2 H(\mu^{cr}/M^0) = 0. \quad (32)$$

In the limit  $M^0 \rightarrow 0$ , we find  $\tilde{\mu}^{cr} = 1/2e^{-\gamma_E/2} \simeq 0.375\dots$  with  $\gamma_E$  being Euler's constant and  $\tilde{\mu} = \mu/\Lambda$  in the PTR scheme. Note that this is only a *sufficient* condition for the existence of DCDW phase, and we can *never* exclude the possibility of the first order phase transition or metamagnetism [6, 11]. Actually, we shall see that DCDW occurs as a first-order phase transition.

### 3.4 First-order phase transition

The magnitudes of  $M$  and  $q$  are obtained from the minimum of the thermodynamic potential (22) for  $T = 0$ . Fig. 6 shows the contours of  $\Omega_{\text{tot}}$  in  $M$ - $q$  plane as the chemical potential

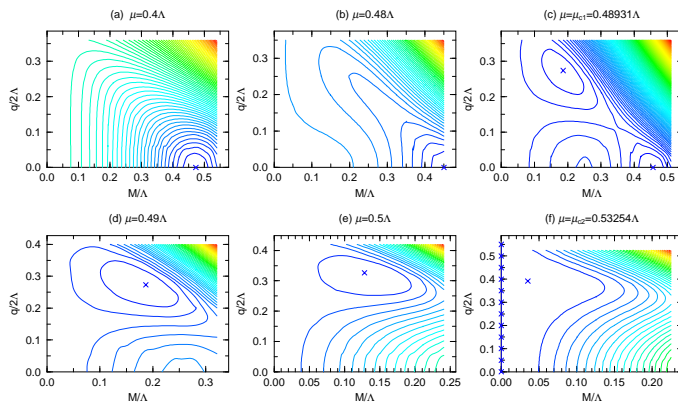


Figure 6: Contours of  $\Omega_{\text{total}}$  at  $T = 0$  are shown in  $M - q$  plane as the chemical potential increases, (a)  $\rightarrow$  (f). The cross in each figure denotes the absolute minimum.

increases, where the parameters are set as  $G\Lambda^2 = 6$  and  $\Lambda = 850$  MeV, which are not far from those for the vacuum ( $\mu = 0$ ) [28].

The crossed points denote the absolute minima. There are two critical chemical potential  $\mu = \mu_{c1}, \mu_{c2}$ : for the lower densities (Fig. 6(a)-(b)) the absolute minimum resides at the point ( $M \neq 0, q = 0$ ) indicating the SSB phase. At  $\mu = \mu_{c1}$  (Fig. 6(c)) the potential has the two absolute minima at ( $M \neq 0, q = 0$ ) and ( $M \neq 0, q \neq 0$ ), showing the first-order transition to the DCDW phase which is stable for  $\mu_{c1} < \mu < \mu_{c2}$  (Fig. (6)d-e). At  $\mu = \mu_{c2}$  (Fig. 6(f)) the axis of  $M = 0$  and a point ( $M \neq 0, q \neq 0$ ) become minima, the system undergoes the first-order transition again to the chiral-symmetric phase.

Fig. 7 shows the behaviors of the order-parameters  $M$  and  $q$  as functions of  $\mu$  at  $T = 0$ , where that of  $M$  without DCDW is also shown for comparison. It is found from the figure that DCDW develops at finite range of  $\mu$  ( $\mu_{c1} \leq \mu \leq \mu_{c2}$ ), where the wave number  $q$  increases with  $\mu$ , which value is smaller than twice of the Fermi momentum  $2k_F (\simeq 2\mu$  for free quarks) due to the higher dimensional effect; the nesting of Fermi surfaces is incomplete in the present 3-D system. Actually, the ratio of the wave number and the Fermi momentum (at normal phase  $q = M = 0$ ) becomes  $q/k_F = 1.17 - 1.47$  for the baryon-number densities  $\rho_b/\rho_0 = 3.62 - 5.30$  where the DCDW is stable (see Fig. 8).

### 3.5 Magnetic properties

The mean-value of the spin operator is given by

$$\bar{s}_z = \frac{1}{2} u_W^\dagger \Sigma_z u_W = \frac{1}{2} \frac{q/2 \pm \beta}{E_p^\pm} + \text{vac}, \quad (33)$$

with  $\beta = \sqrt{p_z^2 + m^2}$ , where "vac" means the vacuum contribution. First note that the integral of  $\bar{s}_z$  over the Fermi seas should be proportional to  $q$ , and the solution with  $q \neq 0$  seems to imply FM. However, we can show that PTR gives the vacuum (the Dirac sea) contribution oppositely to cancel the total mean-value of the spin operator, which is consistent with Eq. (23). Instead we can see that the magnetization spatially oscillates,

$$M_z \equiv \langle \bar{q} \sigma_{12} q \rangle = \langle \gamma_0 \sigma_{12} \rangle \cos(\mathbf{q} \cdot \mathbf{r}), \quad (34)$$

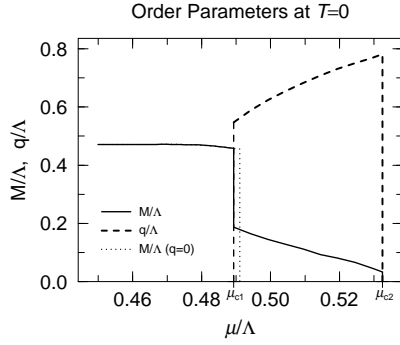


Figure 7: Wave number  $q$  and the dynamical mass  $M$  are plotted as functions of the chemical potential at  $T = 0$ . Solid (dotted) line for  $M$  with (without) the density wave, and dashed line for  $q$ .

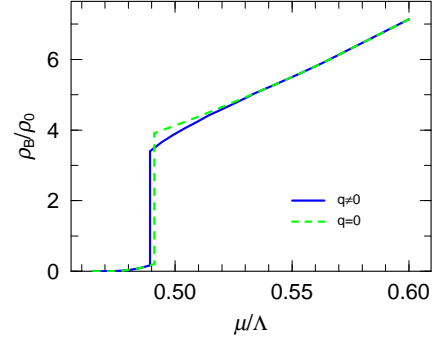


Figure 8: Baryon number density as a function of  $\mu$ .  $\rho_0 = 0.16\text{fm}^{-3}$ : the normal nuclear density.

with

$$\langle \gamma_0 \sigma_{12} \rangle = \int_{F^+ - F^-} \frac{d^3 p}{(2\pi)^3} \frac{2M}{\sqrt{M^2 + p_z^2}}, \quad (35)$$

which means a kind of spin density wave [30].

### 3.6 Phase diagram at $T - \mu$ plane

To complete the phase diagram we derive the thermodynamic potential at finite temperature in the Matsubara formalism. The partition function for the mean-field Hamiltonian is given by

$$\begin{aligned} Z_\beta &= \int D\bar{\psi} D\psi \exp \int_0^\beta d\tau \int d^3 r \left\{ \bar{\psi} \left[ i\tilde{\partial} + M \exp(i\gamma_5 \mathbf{q} \cdot \mathbf{r}) - \gamma_0 \mu \right] \psi - \frac{M^2}{4G} \right\} \\ &= \prod_{\mathbf{k}, n, s=\pm} \left\{ (i\omega_n + \mu)^2 - E_s^2(\mathbf{k}) \right\}^{N_f N_c} \times \exp \left\{ - \left( \frac{M^2}{4G} \right) V \beta \right\}, \end{aligned} \quad (36)$$

where  $\beta = 1/T$ ,  $\tilde{\partial} \equiv -\gamma_0 \partial_\tau + i\gamma \nabla$  and  $\omega_n$  the Matsubara frequency. Thus the thermodynamic potential  $\Omega_\beta$  is obtained,

$$\begin{aligned} \Omega_\beta(q, M) &= -T \log Z_\beta(q, M)/V \\ &= -N_f N_c \int \frac{d^3 \mathbf{k}}{(2\pi)^3} \sum_s \left\{ T \log \left[ e^{-\beta(E_s(\mathbf{k}) - \mu)} + 1 \right] \left[ e^{-\beta(E_s(\mathbf{k}) + \mu)} + 1 \right] + E_s(\mathbf{k}) \right\} + \frac{M^2}{4G}. \end{aligned} \quad (37)$$

From the absolute minima of the thermodynamic potential (37), it is found that the order parameters at  $T \neq 0$  behave similarly to those at  $T = 0$  as a function of  $\mu$ , while the chemical-potential range of the DCDW at finite temperature,  $\mu_{c1}(T) \leq \mu \leq \mu_{c2}(T)$ , gets smaller as  $T$  increases. We show the resultant phase diagram in Fig. (9), where the ordinary chiral-transition line is also given. Comparing phase diagrams with and without  $q$ ,

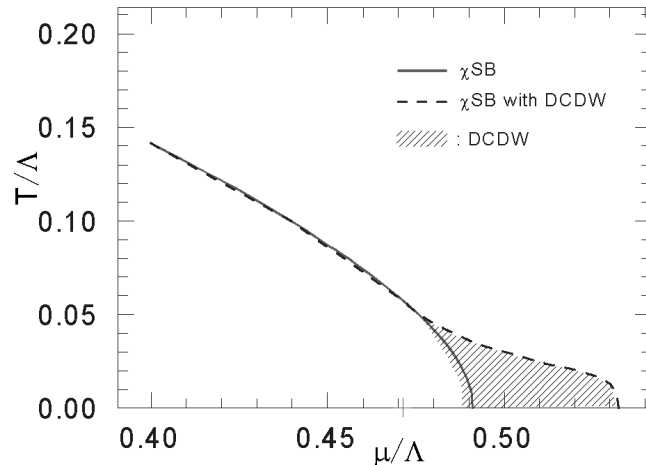


Figure 9: Phase diagram obtained from the thermodynamic potential (37). The solid (dashed) line shows the chiral-restoration line in the presence (absence) of DCDW. The shaded area shows the DCDW phase.

we find that the DCDW phase emerges in the area (shaded area in Fig. (9)) which lies just outside the boundary of the ordinary chiral transition. We thus conclude that the DCDW is induced by finite-density contributions, and has an effect to expand the chiral-condensed phase ( $M \neq 0$ ) toward low temperature and high density region.

## 4 Summary and Concluding remarks

We have seen some magnetic aspects of quark matter: ferromagnetism at high densities and spin density wave at moderate densities within the zero-range approximation for the interaction vertex. These look to follow the similar development about itinerant electrons: Bloch mechanism at low densities and spin density wave at high densities by Overhauser.

With the OGE interaction, we have seen ferromagnetism in quark matter at low densities (Sect.2.1) . It would be worth mentioning that another study with higher-order diagrams also supports it. These studies suggest an opposite tendency to the one using the zero-range interaction (Sects 2.2,2.3). Note that we can also see the same situation for the itinerant electrons; the Hartree-Fock calculation based on the infinite-range Coulomb interaction favors ferromagnetism at low density region, while the Stoner model, which introduces the zero-range effective interaction instead of the Coulomb interaction, gives ferromagnetism at high densities. So we must carefully examine the possibility of ferromagnetim in quark matter by taking into account the finite-range effect.

We have seen that dual chiral desnity wave (DCDW) appears at a certain density and develops at moderate densities (Sect. 3). It occurs as a result of the interplay between the  $\bar{q}q$  and particle-hole correlations. The phase transition is of weakly first order, and the restoration of chiral symmetry is delayed compared with the usual scenario. Note that there is no soft pions in this phase, and phason may appear istead as a Nambu-Goldstone boson.

For the discussion of DCDW, we have seen the remarkable roles of the Fermi sea and the

Dirac sea: the former always favors DCDW, while the latter works against it. The similar situation also appears about the magnetic property of quark matter. The mean value of the spin operator over the Fermi seas of valance quarks always gives a finite value in the presence of DCDW, which is a kind of ferromagnetism, but the vacuum contribution given by the Dirac seas completely cancels it. As a result there is no net spin polarization in this case, but we have seen magnetization spatially oscillates instead (spin density wave). This is one of the typical examples in which the nonrelativistic picture is qualitatively different from the relativistic one by the vacuum effect.

It would be ambitious to give a scenario based on ferromagnetism of quark matter, which can explain the hierarchy of the magnetic field observed in three classes of neutron stars, magnetars, radio pulsars and recycled millisecond pulsars. It would be also interesting to study some implication of spin density wave or phason on the magnetic properties of compact stars.

## Acknowledgments

This work is partially supported by the Grant-in-Aid for the 21st Century COE “Center for the Diversity and Universality in Physics ” from the Ministry of Education, Culture, Sports, Science and Technology of Japan. It is also partially supported by the Japanese Grant-in-Aid for Scientific Research Fund of the Ministry of Education, Culture, Sports, Science and Technology (13640282, 16540246).

## References

- [1] For a review, G. Chanmugam, *Annu. Rev. Astron. Astrophys.* **30** (1992) 143.
- [2] P.M. Woods and C.J. Thompson, *astro-ph/0406133*.
- [3] A.I. Ibrahim et al., *Astrophys. J.* **574** (2002) L51  
N. Rea et al., *Astrophys. J.* **586** (2003) L65.  
G.F. Bignami et al., *astro-ph/0306189*.
- [4] K. Makishima, *Prog. Theor. Phys. Suppl.* **151** (2003) 54.
- [5] For recent results, S. Fantoni et al., *Phys. Rev. Lett.* **87** (2001) 181101; I. Vidana and I. Bombaci, *Phys. Rev.* **C66** (2002) 045801.
- [6] T. Tatsumi, *Phys. Lett.* **B489** (2000) 280.
- [7] D.V. Deryagin, D. Yu. Grigoriev and V.A. Rubakov, *Int. J. Mod. Phys.* **A7** (1992) 659.
- [8] B.-Y. Park, M.Rho, A.Wirzba and I.Zahed, *Phys. Rev.* **D62** (2000) 034015.  
R. Rapp, E.Shuryak and I. Zahed, *Ohys. Rev.* **D63** (2001) 034008.
- [9] R. E. Peierls, *Quantum Theory of Solids* (Oxford University Press, London, 1955).
- [10] A.W. Overhauser, *Phys. Rev.* **128** (1962) 1437.

- [11] F. Bloch, Z. Phys. **57** (1929) 545;
- [12] K. Yoshida, *Theory of magnetism* Springer, Berlin, 1998.
- [13] D.M. Ceperley and B.J. Alder, Phys. Rev. Lett. **45** (1980) 566.  
D.P. Young et al., Nature **397** (1999) 412.
- [14] A. Niegawa, hep-ph/0404252.
- [15] E. Nakano, K. Nawa and T. Tatsumi, in preparation.
- [16] D. Bailin and A. Love, Phys. Reports 107(1984) 325.  
As recent reviews, M. Alford, hep-ph/0102047; K. Rajagopal and F. Wilczek, hep-ph/0011333; D.H. Rischke, Prog. Part. Nucl. Phys. **52** (2004) 197.
- [17] J. Berges and K. Rajagopal, Nucl. Phys. **B538** (1999) 215.
- [18] E. Nakano, T. Maruyama and T. Tatsumi, Phys. Rev. **D68** (2003) 105001; T. Tatsumi, T. Maruyama and E. Nakano, Prog. Theor. Phys. Suppl. **153** (2004) 190; hep-ph/0312351.
- [19] L.N. Buaevskii et al., Adv. Phys. **34** (1985) 175.
- [20] S.S. Sexena et al., Nature **406** (2000) 587; C.Pfleiderer et al., Nature **412** (2001) 58; N.I.Karchev et al., Phys. Rev. Lett. **86** (2001) 846.
- [21] A. J. Leggett, Rev. Mod. Phys. 47 (1975) 331.
- [22] R. Tamagaki, Prog. Theor. Phys. **44** (1970) 905; M. Hoffberg, A.E. Glassgold, R.W. Richardson and M. Ruderman, Phys. Rev. Lett. **24** (1970) 775.
- [23] T. Tatsumi and E. Nakano, hep-ph/0408294; E. Nakano and T. Tatsumi, hep-ph/0411350.
- [24] T. Eguchi and H. Sugawara, Phys. Rev. **D10** (1974) 4257.  
K. Kikkawa, Prog. Theor. Phys. **56** (1974) 947.
- [25] F. Dautry and E.M. Nyman, Nucl. Phys. **319** (1979) 323.  
K. Takahashi and T. Tatsumi, Phys. Rev. **C63** (2000) 015205; Prog. Theor. Phys. **105** (2001) 437.
- [26] M. Kutschera, W. Broniowski and A. Kotlorz, Nucl. Phys. **A516** (1990) 566.
- [27] M. Sadzikowski and W. Broniowski, Phys. Lett. **488** (2000) 63.  
M. Sadzikowski, Phys. Lett. **553** (2003) 45.
- [28] S.P. Klevansky, Rev. Mod. Phys. **64** (1992) 649.  
T. Hatsuda and T. Kunihiro, Phys. Rep. **247** (1994) 221.
- [29] J. Schwinger, Phys. Rev. **92** (1951) 664.
- [30] G. Grüner, Rev. Mod. Phys. **66** (1994) 1.